

# A Design of a Multiband Microstrip Patch Antenna for Ultra-Wideband Applications

**Arijit Das<sup>1</sup>, Avijit Swarnakar<sup>1</sup>, Prodyuti Sarkar<sup>2</sup>, Debasree Chanda (Sarkar)<sup>1</sup>, Sushanta Biswas<sup>1</sup>, Partha Pratim Sarkar<sup>1</sup>**

<sup>1</sup>Department of Engineering & Technological Studies, University of Kalyani, Kalyani, West Bengal, India.

<sup>2</sup>School of bio science and engineering, Jadavpur University, Jadavpur, West Bengal, India.

Corresponding author: Partha Pratim Sarkar

## ABSTRACT

This paper presents the design and analysis of a novel microstrip patch antenna featuring a half-moon-shaped radiating element with dual-port excitation. The proposed structure achieves ultra-wideband (UWB) performance without any modification to the ground plane. Traditional broadband designs typically rely on altered or defected ground configurations. Simulated results demonstrate wide impedance bandwidths, with  $-10\text{dB } S_{11}$  ranging from 10.24 GHz to 36.00 GHz and  $S_{22}$  spanning from 12.6 GHz to 29.80 GHz. Notably, the absence of ground modification does not degrade the radiation performance; the antenna maintains a stable radiation pattern across the operating frequency range with acceptable gain levels. To ensure accuracy and result validation, simulations were performed, showing excellent agreement. The ability to achieve such broadband characteristics through patch geometry alone—without impacting radiation behavior—highlights the antenna's potential for high-frequency UWB applications. Simulated results have been compared with measured Results for verification. They are in Good Parity.

**Keywords:** Microstrip antenna, slot antenna, wide bandwidth, Half-moon.

## 1. INTRODUCTION

The Microstrip Antennas play a crucial role in modern and future wireless communication systems, particularly in supporting high-speed, high-frequency applications[1]. In recent years, ultra-wideband (UWB) antennas have gained significant attention due to their ability to operate over broad frequency ranges, offering advantages such as high data rates and low power consumption. Various antenna configurations—such as monopole antennas[2], [3], [4], defected ground plane antennas[5], [6], [7], [8], partial ground structures[9], [10], and fractal ground geometries[11], [12]—have been widely explored to achieve UWB performance. However, these approaches typically rely on ground plane modifications, which often introduce undesirable back radiation and degrade the radiation pattern. To compensate these effects, frequency selective surfaces (FSS) may be integrated to suppress back radiation and stabilize radiation performance. While effective, the use of FSS significantly increases both the physical size and manufacturing cost of the antenna system.

In this work, we propose a novel antenna structure that eliminates the need for any ground plane modification or external FSS. The antenna features a half-moon shaped metallic patch mounted on a lossy FR4 substrate and is excited through two ports. Despite its simple geometry, the design achieves ultra-wideband performance with  $S_{11}$  covering X to Ka band (10.24 GHz to 36.00 GHz) and  $S_{22}$  spanning from Ku to Ka band (12.6 GHz to 29.80 GHz). Importantly, the antenna maintains a stable radiation pattern with acceptable gain across the entire frequency range, without generating significant

back radiation. This compact and cost-effective design is well-suited for various high-frequency UWB applications.

## 2. ANTENNA STRUCTURE

The proposed antenna is constructed on an FR4 lossy substrate with a dielectric constant of 4.4. The substrate is square type and has dimensions of  $50 \text{ mm} \times 50 \text{ mm}$  along the X and Y directions and a thickness of 1.6 mm. A perfect electric conductor (PEC) is used as the radiating patch material, with a metal thickness of 0.02 mm. The ground plane is placed on the bottom side of the substrate and has the same dimensions as the substrate, i.e.,  $50 \text{ mm} \times 50 \text{ mm}$ .

To form the radiating patch, a geometric method is employed. First, a circle with a radius of 20 mm is drawn on the substrate. Along one of its radii, a point is marked at a distance of 31.7 mm from the centre of this circle. Using this point as a new centre, a second circle with a radius of 38 mm is drawn. The two circles partially overlap, creating a distinct composite shape. The overlapped region is treated as a slot, while the remaining portion of the smaller (20 mm radius) circle forms a half-moon shaped structure. This half-moon shaped area is used as the radiating patch in the proposed antenna. Dimension and actual Shape are shown in Figure 1(a).

The antenna is excited using a dual-port configuration to analyze its wideband behavior and port isolation. The complete geometry including substrate, ground, and patch formation is illustrated in Figure 1(b, c)

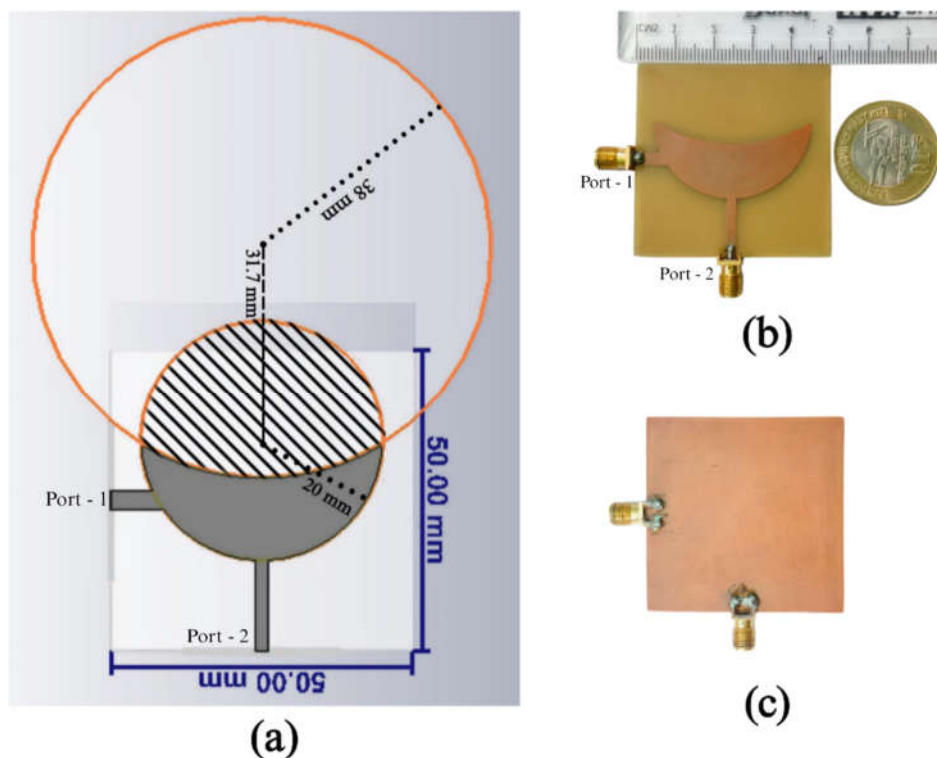


**Figure 1.** (a) Geometry of the proposed dual-port half-moon shaped UWB microstrip patch antenna. Fabricated prototype of the proposed antenna: (b) Top view showing the half-moon patch and feed ports, (c) Bottom view showing the full ground plane.

## 3. EXPERIMENTAL VALIDATION AND COMPARATIVE ANALYSIS OF SIMULATED AND MEASURED RESULTS

To validate the simulation results, real-time measurements were carried out in the institutional microwave laboratory using standard microwave test bench, as shown in Figure 2

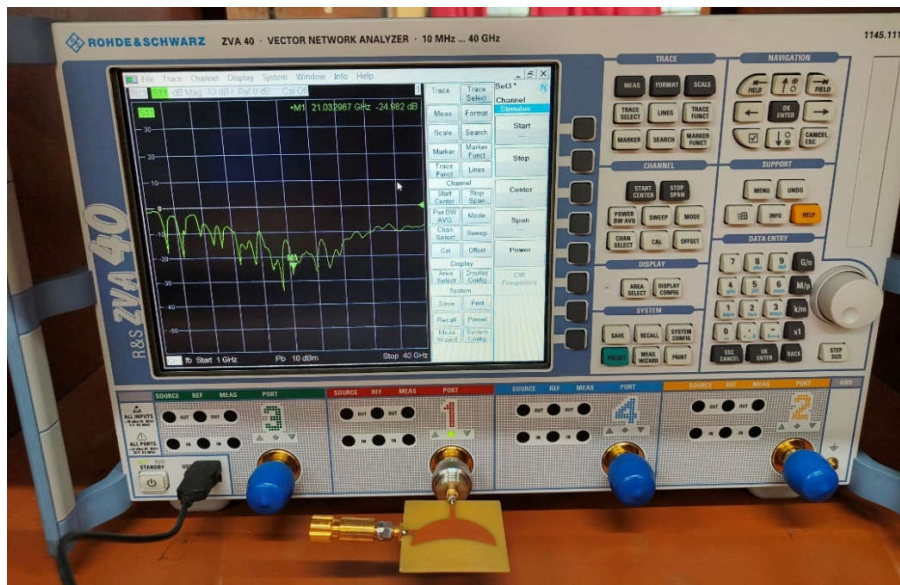


**Figure 2.** Vector Network Analyzer (VNA) setup used for measuring the reflection coefficients ( $S_{11}$  and  $S_{22}$ ) of the fabricated antenna.

The simulated and Measured S-parameter results are shown in Figure 3, where during the simulation of  $S_{11}$ , Port 2 was terminated with a matched load, and similarly, while simulating  $S_{22}$ , Port 1 was terminated with a matched load. From the  $S_{11}$  plot, several operating bands were obtained. The first operating band appears from 3.3 GHz to 3.5 GHz with a resonant frequency at 3.4 GHz. The second band is observed between 7.43 GHz and 7.816 GHz, with a resonant frequency at 7.6 GHz. The third band lies between 8.83 GHz and 9.48 GHz, and the resonant frequency is 9.2014 GHz. The fourth operating band ranges from 10.31 GHz to 12.07 GHz with a resonant frequency at 11.60 GHz. The fifth and widest operating band spans from 12.86 GHz to 36.00 GHz, where the reflection coefficient remains consistently below  $-10$  dB. The resonant frequency in this band is found at 20.79 GHz. The simulation was performed up to 36 GHz.

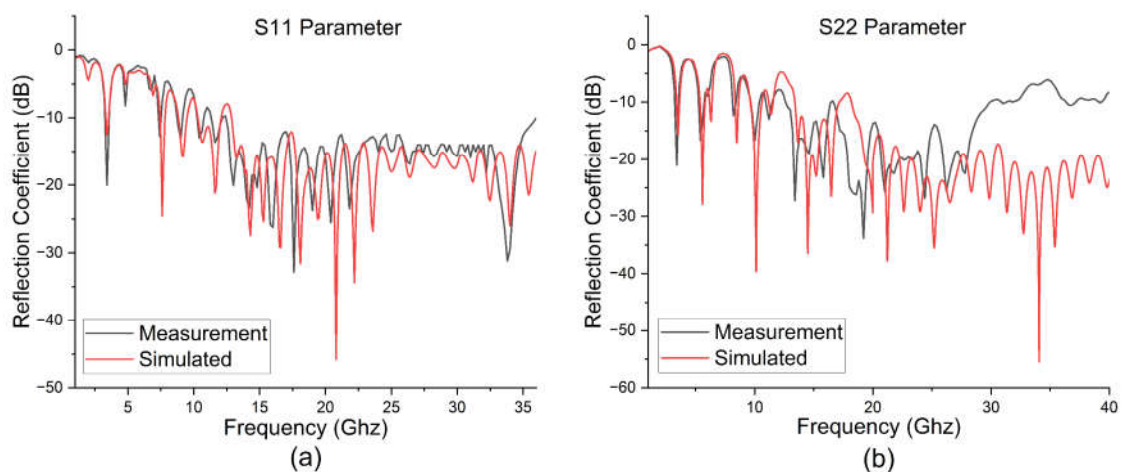


**Figure 3.** Comparison of simulated and measured S-parameters: (a)  $S_{11}$ , (b)  $S_{22}$ .

From the S22 result, multiple operating bands were also observed. The first band ranges from 3.39 GHz to 3.64 GHz with a resonant frequency at 3.52 GHz. The second band appears from 5.37 GHz to 5.80 GHz, and another resonant frequency is present between 8.35 GHz and 8.64 GHz, with a reflection coefficient minimum at 8.5 GHz. The third band ranges from 9.63 GHz to 10.6 GHz with a resonant frequency at 10.1 GHz. The fourth band appears from 13.4 GHz to 17.14 GHz with a resonant frequency at 14.49 GHz. The fifth operating band starts from 18.18 GHz, and the resonant frequency is observed at 34.06 GHz. Although the simulation was carried out up to 40 GHz, the reflection coefficient continues to stay below  $-10$  dB, and the frequency range was not further increased as the available VNA supports a frequency range of 100 MHz to 40 GHz.

The measured & Simulated S-parameters, as shown in Figure 3, exhibit good agreement with the simulated results. The resonant frequency frequencies observed in the measurements closely match the simulated values, with only negligible differences. Both S11 and S22 remain below  $-10$  dB across multiple frequency bands, confirming the broadband nature of the antenna and validating the reliability of the proposed design.

### 3.1 Radiation pattern analysis and experimental validation

The comparison and analysis of simulated and measured radiation patterns at multiple frequencies are illustrated in Figure 4. At each selected frequency, the measured radiation pattern closely matches the simulated plot, demonstrating good agreement and validating the design's performance. It is important to note that the radiation pattern measurements were limited to frequencies below 18.5 GHz, as the power meter used during the experiment supports measurements only up to this frequency range.

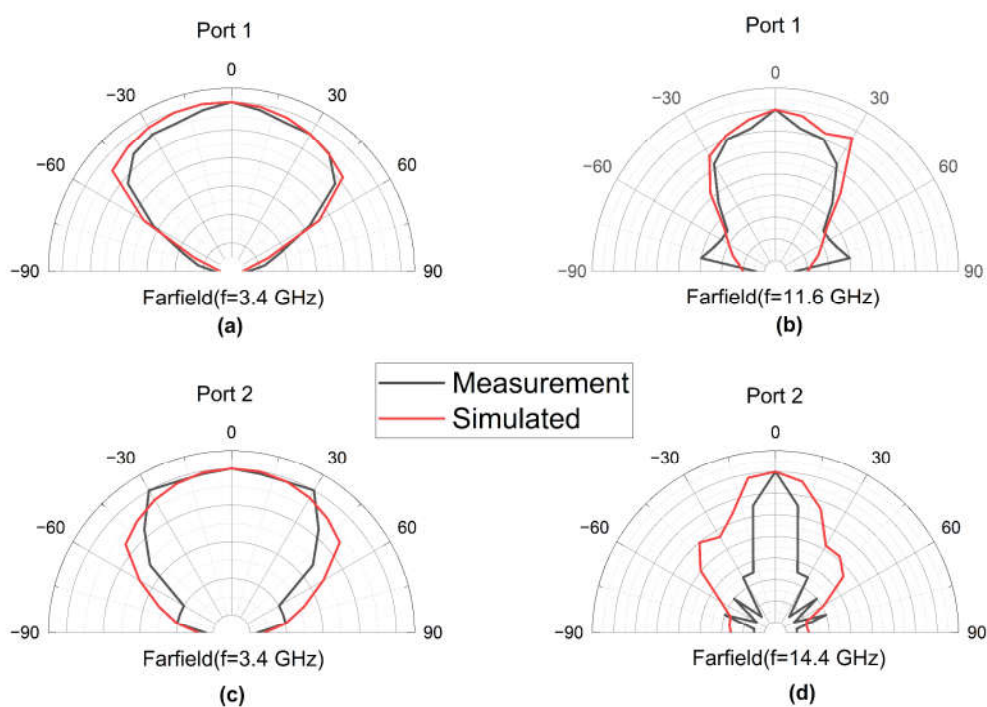


**Figure 4.** Simulated vs Measurement radiation patterns of the proposed antenna at selected frequencies: (a) Port 1 at 3.4 GHz, (b) Port 1 at 11.6 GHz, (c) Port 2 at 3.4 GHz and, (d) Port 2 at 14.4 GHz

The simulated and measured radiation patterns are shown in Figure 4. In all the evaluated cases, the main lobe was observed to be stronger than the back lobe, indicating desirable directional radiation

characteristics. Therefore, the radiation patterns can be considered suitable for practical applications. The front-to-back ratio (FBR) was calculated at several key frequencies. At 3.4 GHz, the FBR was found to be 11.84 dB; at 11.6 GHz, it was 9.52 dB; and at 14.4 GHz, it was 10.57 dB.

### 3.2 Gain measurement and validation with simulated results

The simulated gain performance of the proposed antenna is presented in Figure 5 (a). It can be observed that the antenna exhibits positive gain throughout the majority of its operational bandwidth. Simulated and measured gain in dBi have been plotted in the same graph for comparison. It is important to note here that at the time of gain measurement Port 1 was terminated by matched load of  $50\ \Omega$  and the Power meter was connected to the Port 2 through Power sensor. It is important to note that the gain measurements were limited to frequencies below 18.5 GHz due to the frequency range limitation of the power meter used in the experiment. Further, the reference antenna required for gain comparison operates within the range of 3.2 GHz to 13.2 GHz. As a result, the measured gain has been plotted for the frequency range of 3.5 GHz to 11.6 GHz, as shown in Figure 5(b).

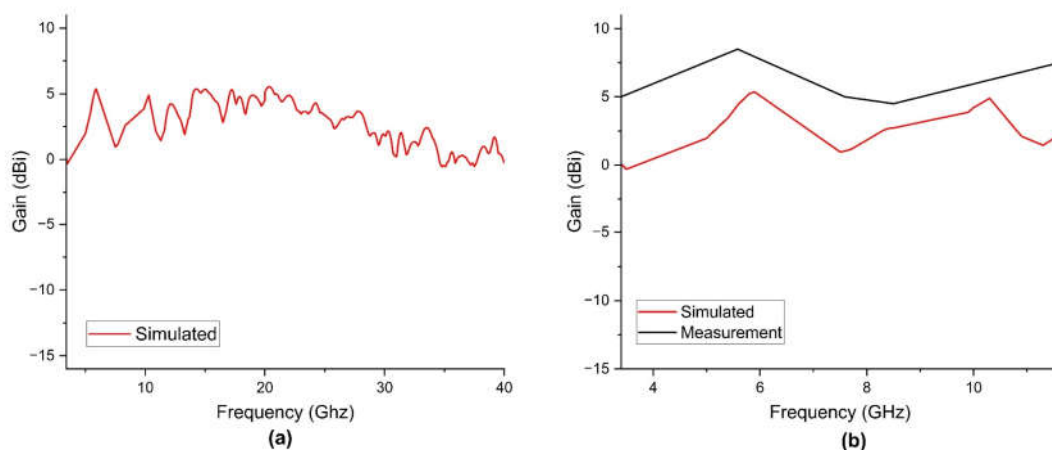


**Figure 5.** (a) Simulated Gain of the proposed antenna up to 40GHz, (b) Simulated and Measured Gain

## 4. CONCLUSION

In this research work, a dual-port microstrip antenna has been successfully designed, simulated, and experimentally validated. The novelty of the proposed design lies in achieving an ultra-wide bandwidth of approximately 134% without modifying the ground plane and without compromising the antenna's radiation characteristics or gain performance. The measured results exhibit agreement with simulation, and the antenna demonstrates stable radiation patterns across the operating bands. The highest measured gain reaches up to 8.5 dBi. All the operating bands obtained from this design may be well applied in 5G WiMAX and different satellite communication applications.

## 5. REFERENCES

- [1] M. Rana and S. Islam, "Microstrip Patch Antenna Design and Simulation for Wireless Communication Systems Operating at 3.5GHz," *Indones. J. Electr. Eng. Inform. IJEEI*, vol. 10, pp. 943–952, Jan. 2023, doi: 10.52549/ijeei.v10i4.4141.
- [2] W. Ali, A. Ibrahim, and J. Machac, "Compact Size UWB Monopole Antenna with Triple Band-Notches," *Radioengineering*, vol. 26, pp. 57–63, Apr. 2017, doi: 10.13164/re.2017.0057.
- [3] S. Sakulchat, A. Ruengwaree, V. Thongpool, and W. Naktong, "Low-Cost Flexible Graphite Monopole Patch Antenna for Wireless Communication Applications," *Comput. Mater. Contin.*, vol. 71, pp. 6069–6088, Jan. 2022, doi: 10.32604/cmc.2022.024050.

- [4] F. Y. Zulkifli, A. Wahdiyati, A. Zufar, N. Nurhayati, and E. Setijadi, "Super-Wideband Monopole Printed Antenna with Half-Elliptical-Shaped Patch," *Telecom*, vol. 5, pp. 760–773, Aug. 2024, doi: 10.3390/telecom5030038.
- [5] A. Tsegaye, X.-Q. Lin, H. Liu, and H. S. Abubakar, "A Compact Monopole Wideband Antenna Based on DGS," *Electronics*, vol. 14, no. 12, Art. no. 12, Jan. 2025, doi: 10.3390/electronics14122311.
- [6] P. Kumar *et al.*, "A defected ground structure based ultra-compact wider bandwidth terahertz multiple-input multiple-output antenna for emerging communication systems," *Heliyon*, vol. 10, p. e36842, Sept. 2024, doi: 10.1016/j.heliyon.2024.e36842.
- [7] W. J. Lee, W.-S. Yoon, D. Ahn, and S.-M. Han, "Compact Design Method for Planar Antennas with Defected Ground Structures," *Electronics*, vol. 12, no. 10, Art. no. 10, Jan. 2023, doi: 10.3390/electronics12102226.
- [8] I. Bouchachi *et al.*, "Design and performances improvement of an UWB antenna with DGS structure using a grey wolf optimization algorithm," *Heliyon*, vol. 10, no. 5, p. e26337, Mar. 2024, doi: 10.1016/j.heliyon.2024.e26337.
- [9] L. Paul *et al.*, "A low-profile antenna with parasitic elements and a DGS-based partial ground plane for 5G/WMAN applications," *Discov. Appl. Sci.*, vol. 6, Jan. 2024, doi: 10.1007/s42452-024-05669-9.
- [10] M. A. Abdul Aziz, N. Seman, and T. H. Chua, "Microstrip antenna design with partial ground at frequencies above 20 GHz for 5G telecommunication systems," *Indones. J. Electr. Eng. Comput. Sci.*, vol. 15, p. 1466, Sept. 2019, doi: 10.11591/ijeecs.v15.i3.pp1466-1473.
- [11] R. Karanam and D. Kakkar, "Design and optimization of UWB fractal micro strip patch antenna for vehicular communication applications under futuristic frequencies," *Analog Integr. Circuits Signal Process.*, vol. 122, Jan. 2025, doi: 10.1007/s10470-025-02301-7.
- [12] S. S and T. Bai, "A compact ultra-wide band fractal antenna for breast cancer detection applications," *Alex. Eng. J.*, vol. 103, pp. 376–383, Sept. 2024, doi: 10.1016/j.aej.2024.06.018.
- [13] N. Sharma and V. Sharma, "A design of Microstrip Patch Antenna using hybrid fractal slot for wideband applications," *Ain Shams Eng. J.*, vol. 9, no. 4, pp. 2491–2497, Dec. 2018, doi: 10.1016/j.asej.2017.05.008.
- [14] L. Zhang, Q.-Q. Li, and H.-F. Zhang, "A wideband and high-gain circularly polarized reconfigurable antenna array based on the solid-state plasma," *Eng. Sci. Technol. Int. J.*, vol. 48, p. 101584, Dec. 2023, doi: 10.1016/j.jestch.2023.101584.
- [15] W. Wiesbeck, G. Adamiuk, and C. Sturm, "Basic Properties and Design Principles of UWB Antennas," *Proc. IEEE*, vol. 97, pp. 372–385, Mar. 2009, doi: 10.1109/JPROC.2008.2008838.
- [16] M. Samsuzzaman *et al.*, "Circular slotted patch with defected grounded monopole patch antenna for microwave-based head imaging applications," *Alex. Eng. J.*, vol. 65, pp. 41–57, Feb. 2023, doi: 10.1016/j.aej.2022.10.034.
- [17] A. Abbas, W. A. Awan, N. Hussain, D. Choi, S. Lee, and N. Kim, "Highly selective-notch band ultrawide band antenna: A review," *Heliyon*, vol. 11, no. 2, p. e41922, Jan. 2025, doi: 10.1016/j.heliyon.2025.e41922.
- [18] A. Abbas, N. Hussain, M. A. Sufian, J. Jung, S. M. Park, and N. Kim, "Isolation and Gain Improvement of a Rectangular Notch UWB-MIMO Antenna," *Sensors*, vol. 22, no. 4, Art. no. 4, Jan. 2022, doi: 10.3390/s22041460.
- [19] T. Addepalli *et al.*, "Parameters Optimization of Compact UWB-MIMO Antenna with WLAN Band Rejection for Short Distance Wireless Communication," *IETE J. Res.*, vol. 0, no. 0, pp. 1–17, doi: 10.1080/03772063.2025.2483933.
- [20] S. Maity, T. Tewary, S. Mukherjee, A. Roy, P. P. Sarkar, and S. Bhunia, "Super wideband high gain hybrid microstrip patch antenna," *AEU - Int. J. Electron. Commun.*, vol. 153, p. 154264, Aug. 2022, doi: 10.1016/j.aeue.2022.154264.
- [21] H. Nakano, Y. Yamamoto, M. Seto, K. Hitosugi, and J. Yamauchi, "A half-moon antenna," *IEEE Trans. Antennas Propag.*, vol. 52, no. 12, pp. 3237–3244, Dec. 2004, doi: 10.1109/TAP.2004.836427.